Supporting Material

In vivo imaging-guided nanoplatform for tumor targeting delivery and combined chemo-, gene- and photothermal therapy

Cheng Li[a‡], Xiao-Quan Yang[a‡], Ming-Zhen Zhang[b,c], Yuan-Yang Song[a], Kai Cheng[a], Jie An[a], Xiao-Shuai Zhang[a], Yang Xuan[a], Bo Liu[a], Yuan-Di Zhao[a,d,*]

[a] Britton Chance Center for Biomedical Photonics at Wuhan National Laboratory for Optoelectronics–Hubei Bioinformatics & Molecular Imaging Key Laboratory, Department of Biomedical Engineering, College of Life Science and Technology, Huazhong University of Science and Technology, Wuhan 430074, Hubei, P. R. China

[b] Institute of Medical Engineering, Department of Biophysics, School of Basic Medical Sciences, Xi'an Jiaotong University Health Science Center, Xi'an, Shaanxi, 710061, China

[c] Digestive Disease Research Group (DDRG), Institute for Biomedical Sciences, Center for Diagnostics and Therapeutics, Georgia State University, Atlanta, GA, 30302, USA.

[d] Key Laboratory of Biomedical Photonics (HUST), Ministry of Education, Huazhong University of Science and Technology, Wuhan 430074, Hubei, P. R. China

‡ These authors equally contributed to this article.

* Corresponding author. Tel/Fax: +86-27-8779-2202. Email address: zydi@mail.hust.edu.cn (Y.D. Zhao).

Materials

Diethyldithiocarbamic acid silver salt (Ag(DDTC), 98%), FA (97%), 1-(3-dimethylaminopropyl)-3-ethylenediamine hydrochloride (EDC) and N-hydroxysuccinamide (NHS) were purchased from Aladdin Industrial Co., Ltd. (Shanghai, China); octadecene (ODE, 90%), hexadecyltrimethylammonium bromide (CTAB), tetraethylorthosilicate (TEOS), 3-aminopropyltriethoxysilane (APTES) and desthiobiotin (db) were purchased from Sigma-Aldrich (St. Louis, MO, USA); biotin, avidin and doxorubicin hydrochloride (DOX) were purchased from Sangon Biotech Industrial Co., Ltd. (Shanghai, China); dodecylmercaptan (DT, 98%), *n*-hexane, trichloromethane, acetone, ethyl acetate, ammonium nitrate and dimethyl sulfoxide (DMSO) were purchased from Sinopharm Chemical Reagent Co., Ltd. (Shanghai, China). The anti-survivin antisense oligonucleotide (db-DNA), 5'-desthiobiotin-*CCC*AGCCTTCCAGCTCCT*TG*-3' (italics underlined bases were phosphorothioate-modified) and Carboxyfluorescein (FAM) labeled db-DNA (db-DNA-FAM) were provided by Sangon Biotech Industrial Co., Ltd. (Shanghai, China). All chemicals and reagents were used as received without any further purification.

Characterizations

Probe morphology characterization and element analysis were performed by Tecnai G2 20 U-Twin high resolution transmission electron microscopy (FEI, U.S.) and EDX spectroscopy. The elemental mapping images were performed by Talos F200X Field emission electron microscopy (FEI, U.S.). The absorption spectra were measured by UV-2550 UV-vis spectrophotometer (Shimadzu, Japan). The fluorescence spectra of DOX, Ag_2S QD and Ag_2S@MSN were obtained by LS-55 fluorescence spectrophotometer (PerkinElmer, USA) or QE6500 fiber spectrometer (Ocean Optics, USA). ZS90 ZetaSizer (Malvern, UK) was employed to characterize the size and surface potential of probe, X-ray diffraction (XRD) pattern was recorded by Empyrean XRD (PANalytical B.V., NED) using Cu-Kα

radiation from 1º to 10º, and the specific surface area (BET) and pore size distribution (BJH) of Ag_2S@MSN were analyzed by ASAP 2020 fully automatic surface area analyzer (Micromeritics Instrument, USA). MDL-III-808-2.5 W laser (Changchun New Industries, China) was used for laser irradiation, and thermal imaging was recorded by EasIR-9 infrared thermal imager (Wuhan Guide, China). Near infrared fluorescence imaging system was built up by our laboratory [1].

Cell culture

HeLa cell line was cultured in DMEM culture medium (Gbico, Invitrogen) containing 10% FBS and A549 cell line was cultured in RPMI 1640 culture medium (Gbico, Invitrogen) containing 10% FBS. Antibiotics penicillin (100 U/mL) and streptomycin (100 μg/mL) were added in both medium. All cells were incubated in a humidified atmosphere containing 5% CO_2 at 37 °C.

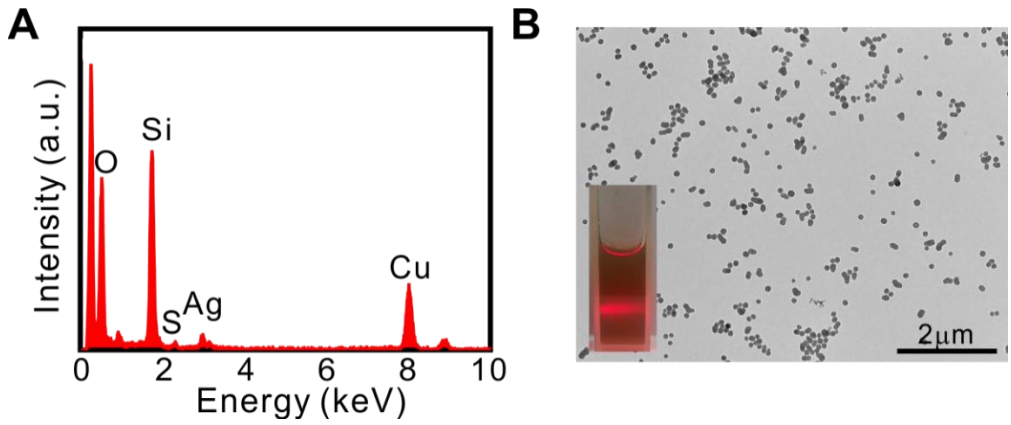

Figure S1. EDX spectrum of QD@M (A); TEM image of QD@M under a large field of view, inset was the Tyndall effect of QD@M (B)

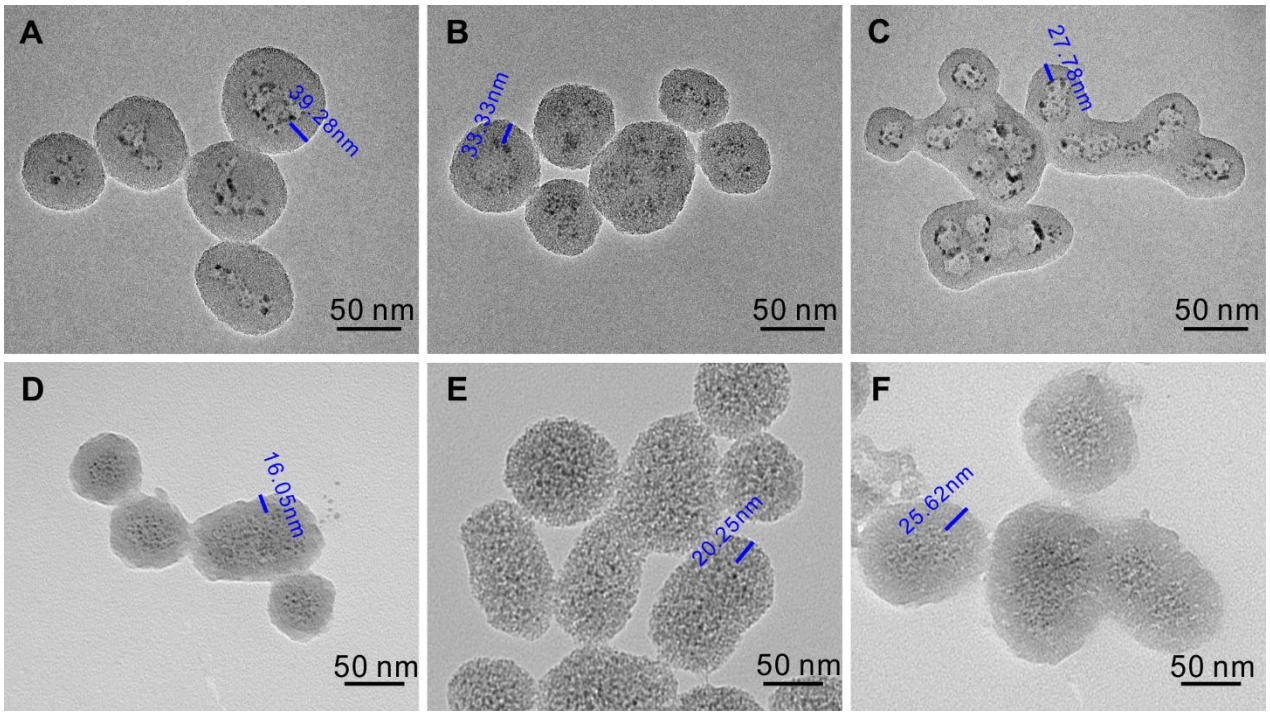

Figure S2. TEM images of QD@M obtained by different amounts of Ag_2S (A-C: 4, 6 and 8 mg) and TEOS (D-F: 300, 400 and 500 μL).

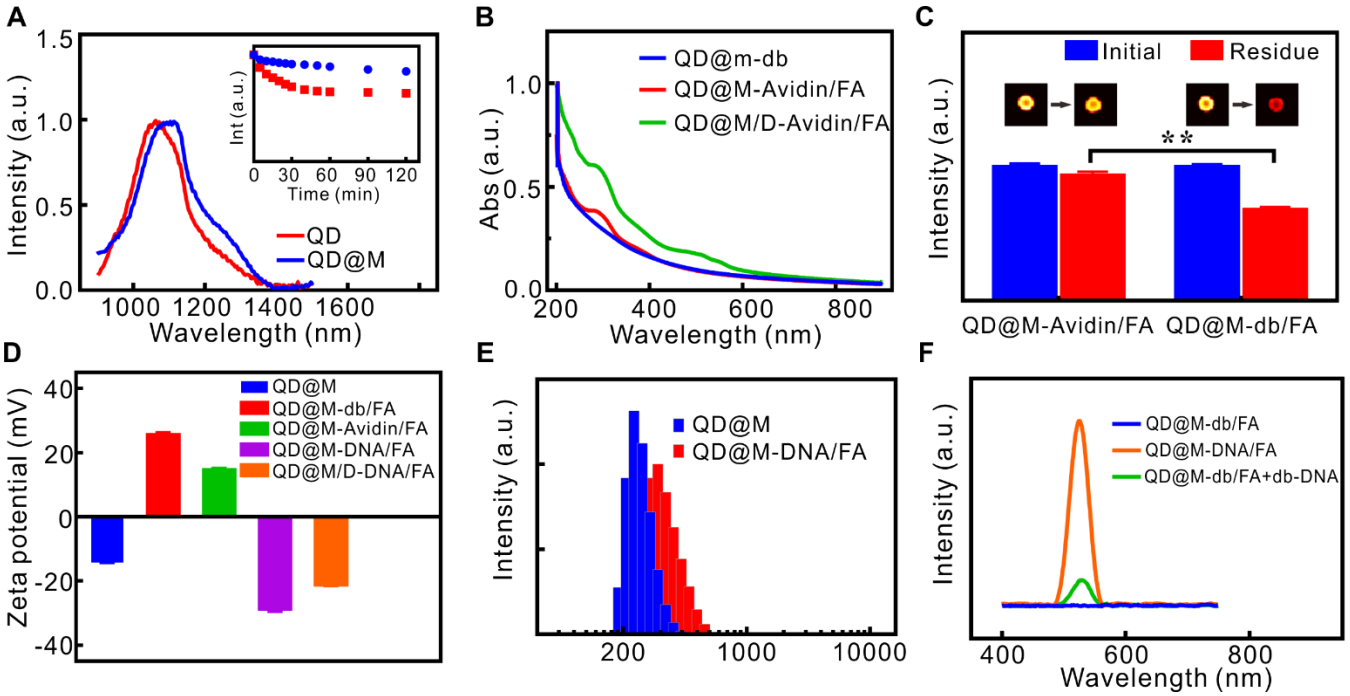

Figure S3. Fluorescence spectra of Ag_2S QD and QD@M (A), and changes of their fluorescence intensities under 808 nm laser irradiation (inset); UV-Vis spectra of QD@M-db, QD@M-Avidin/FA and QD@M/D-Avidin/FA (B); fluorescence changes of db-modified NC membrane after QD@M-Avidin/FA and QD@M-db/FA treatment and cleaning respectively (C); zeta potentials of different nanoparticles (D); hydrated particle size distribution of QD@M and QD@M-DNA/FA (E); fluorescence spectra of QD@M-db/FA, QD@M-DNA/FA, and QD@M-db/FA directly mixed with db-DNA, db-DNA used in the latter two cases was modified by FAM (F). **: $p<0.01$.

Fluorescence spectrum showed that emission of Ag_2S QD was about 1050 nm under 808 nm excitation, and the fluorescence quantum yield was about 8.5±0.74%. However, after mesoporous silica coating, this value reduced to 3.4±0.75% and a slight red shift of emission peak (Figure S3A). This change might be caused by the existence of silicon layer. At the same time, owing to the protection of silicon layer, photo-bleaching resistance of Ag_2S QD after encapsulation was improved (Figure S3A, inset). Amino-functionalized FA and db silane precursors were grafted on the surface of QD@M by silane hydrolysis, and then avidin was coupled to mesoporous silica surface through desthiobiotin-avidin interaction. UV-Vis absorbance spectra showed QD@M-Avidin/FA exhibited a significant FA absorption

peak at 280 nm when compared with QD@M-db, and the characteristic absorption peak of DOX appeared at 590 nm after DOX was loaded (Figure S3B). To verify the introduction of avidin, QD@M-db/FA and QD@M-Avidin/FA with the same concentration were added onto db-modified NC membranes for 2 h respectively, then the membranes were fully washed by water to remove free probes. It was found that fluorescence intensity of NC membrane treated by QD@M-Avidin/FA was almost unchanged while that of QD@M-db/FA was much weaker (Figure S3C, $p<0.01$), indicating QD@M-Avidin/FA was firmly bound to NC membrane due to the presence of avidin. Zeta potential was also used to investigate the surface modification and charge changes of nanoparticles (Figure S3D). It was shown that QD@M had a negative potential (-14.1±0.31 mV) due to hydroxyl groups; when FA and db silane precursor were modified to the surface, the value reversed to 25.5±0.83 mV caused by APTES in the precursor mixture, then to 14.6±0.4 mV after avidin binding to db. Since the isoelectric point of avidin was about 10~10.5, it was speculated that although the macromolecule avidin was positively charged, but its modification on amino silane reduced surface charge density, thus leading to lower zeta potential. After binding the electronegative db-DNA, the value reversed to -28.8±0.9 mV. When DOX was loaded into nanoparticle, a decrease of zeta potential was observed (-21.3±0.3 mV), due to electropositive amine in DOX. The achieved charge of the nanoparticles has been previously shown to be optimal for a long-lasting *in vivo* circulation time. Dynamic Light Scattering (DLS) measurements showed that the particle size increased from 122.4±2.67 nm to 190.1±1.17 nm after binding db-DNA (Figure S3E). TEM also showed that the pore had been covered and no visible mesoporous structure (Figure 2D). Since QD@M-Avidin/FA surface was positively charged, to determine whether negatively charged db-DNA was modified to probe surface by electrostatic adsorption or desthiobiotin-avidin interaction, carboxyfluorescein (FAM) labeled db-DNA was used, it was found that avidin was coupled to probe, the amount of DNA attached to surface was significantly higher than that on avidin unmodified

probe (Figure S3F), indicating that db-DNA was mainly modified to probe surface by desthiobiotin-avidin interaction, and a small amount was also directly adsorbed.

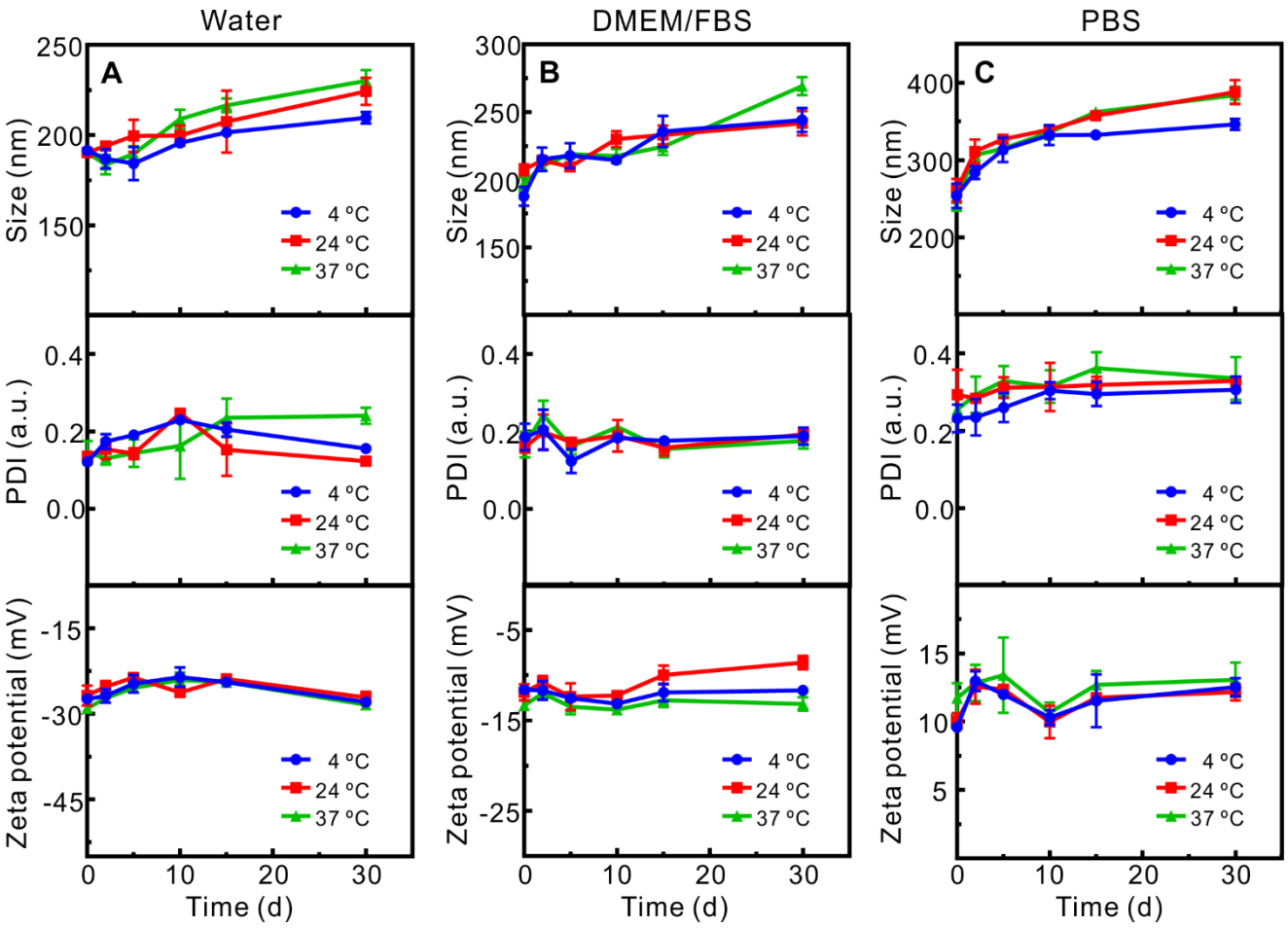

Figure S4. The change of hydrated particle size, PDI and zeta potential of QD@M-DNA/FA stored in water (A), DMEM medium with 10% FBS (B) and PBS (C) at 4, 24 and 37 ºC, respectively.

To further evaluate the stability of the nanoparticle, QD@M-DNA/FA was stored in water, DMEM (10% FBS) medium and PBS respectively at 4, 24 and 37 ºC for 30 d, the results showed that particle size, PDI and zeta potential did not change significantly, illustrating that temperature in the range of 4-37 ºC and storage environment had little effect on QD@M-DNA/FA.

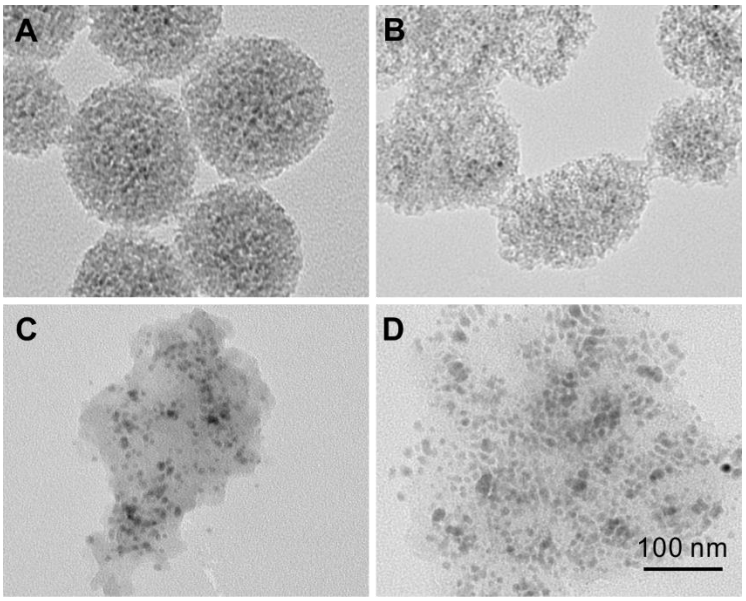

Figure S5. TEM images of QD@M (A) and after incubation in different solutions for 30 d at 37 ºC, serum-containing DMEM (10% FBS) at pH 7.4 (B), PBS at pH 6.5 (C) and pH 5.5 (D).

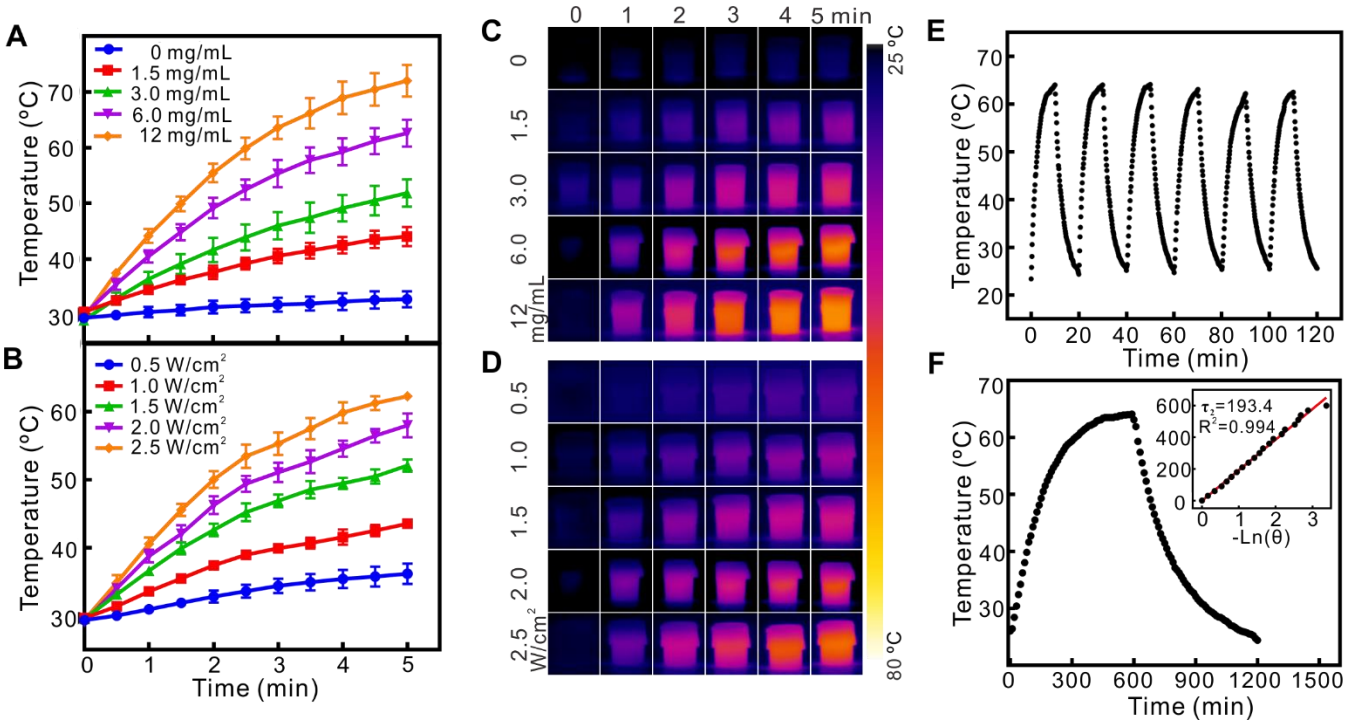

Figure S6. The photothermal ability of QD@M. Photothermal heating curves (A) and infrared thermal images (C) of QD@M at different concentrations under same laser irradiation (1.5 W/cm^2); photothermal heating curves (B) and infrared thermal images (D) of QD@M (3.0 mg/mL) under various power intensities; heating of QD@M in water for six laser on/off cycles with 808 nm laser (2 W/cm^2) (E); heating and cooling curve of QD@M under laser irradiation (F).

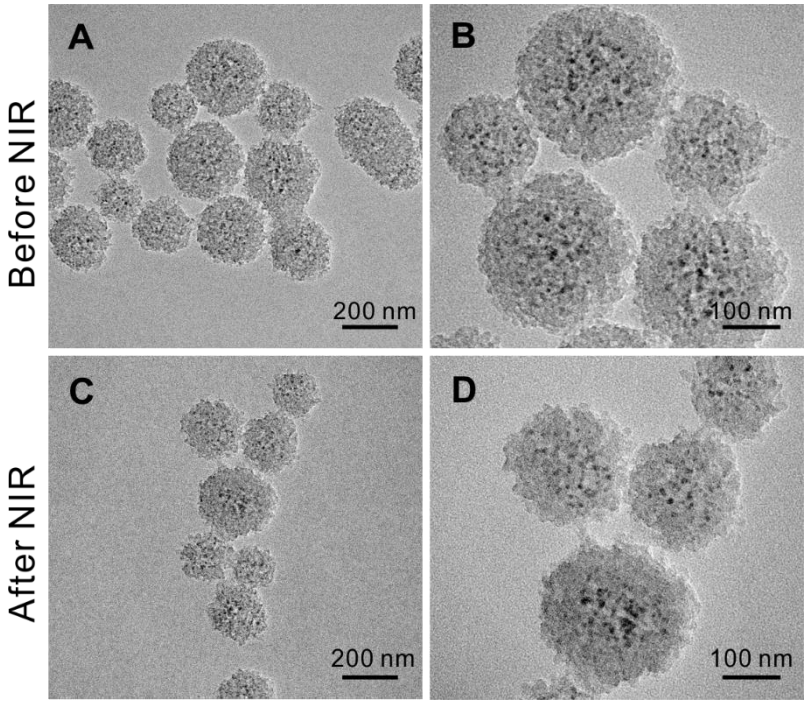

Figure S7. TEM images of QD@M-DNA/FA before and after laser irradiation.

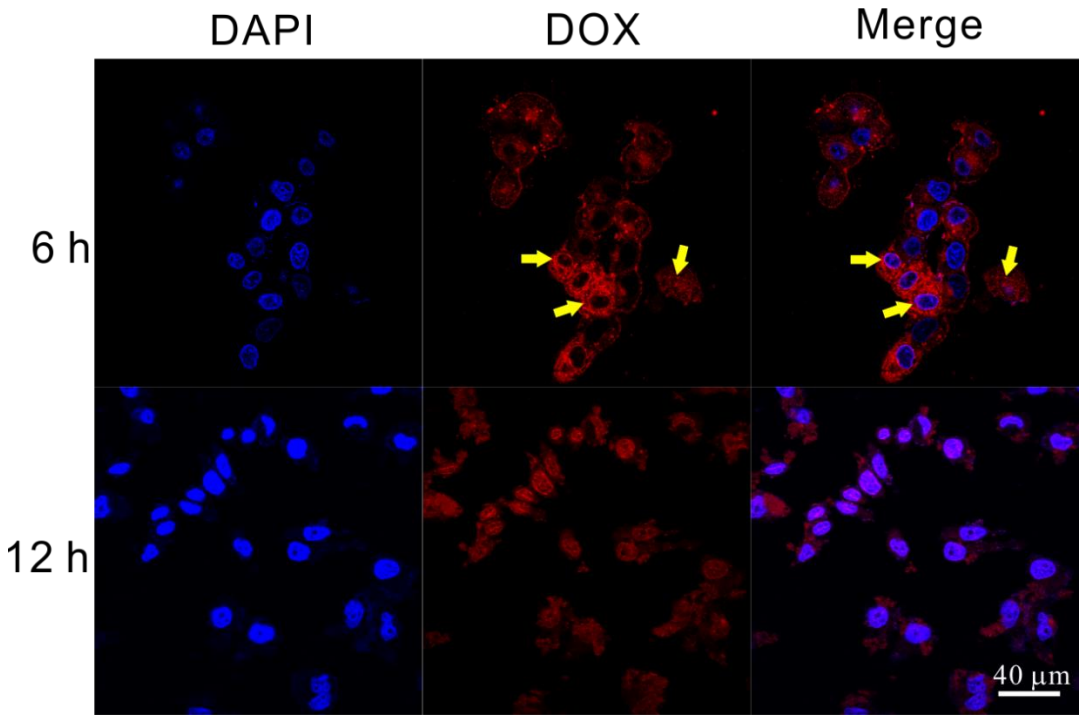

Figure S8. Confocal fluorescence images of HeLa cells for prolonged 6 h and 12 h incubation time after 2 h treatment of QD@M/D-Avidin/FA and refresh medium. The yellow arrow indicates the early nuclear entry signal.

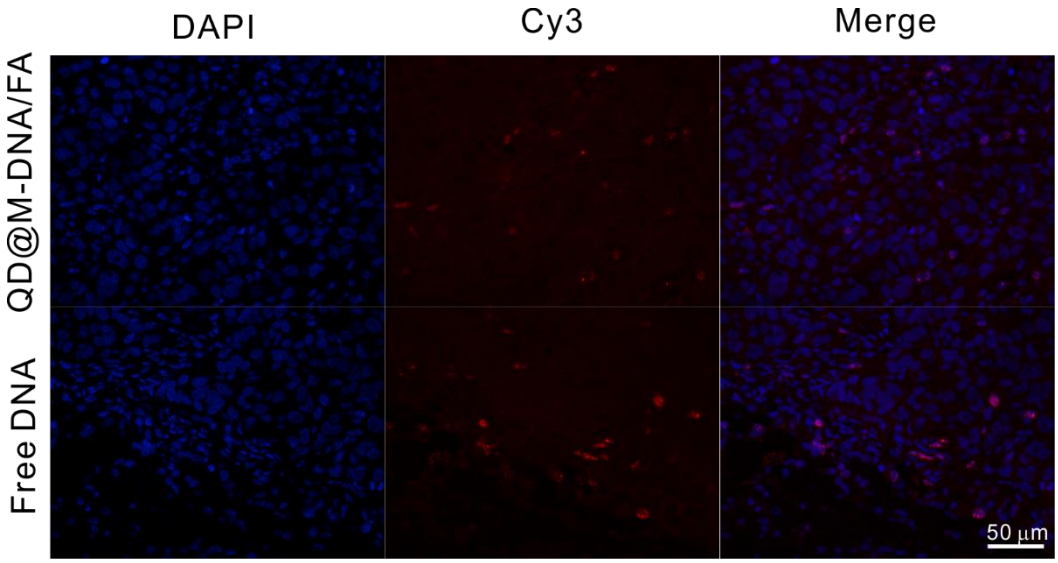

Figure S9. Immunohistochemical (IHC) analysis to explore the inhibition of survivin. Blue was DAPI stained nucleus and red was Cy3 labeled survivin.

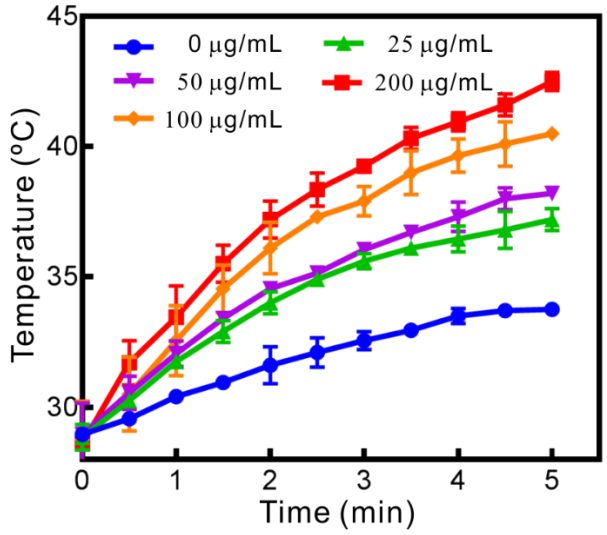

Figure S10. Photothermal heating curves of QD@M at lower concentrations under laser irradiation (2 W/cm^2).

Because the cell experiment used a lower probe concentration, so we studied the photothermal properties of the probe with a lower concentration. As shown in Figure S10, low concentration had potential of cell photothermal therapy under 808 nm laser irradiation.

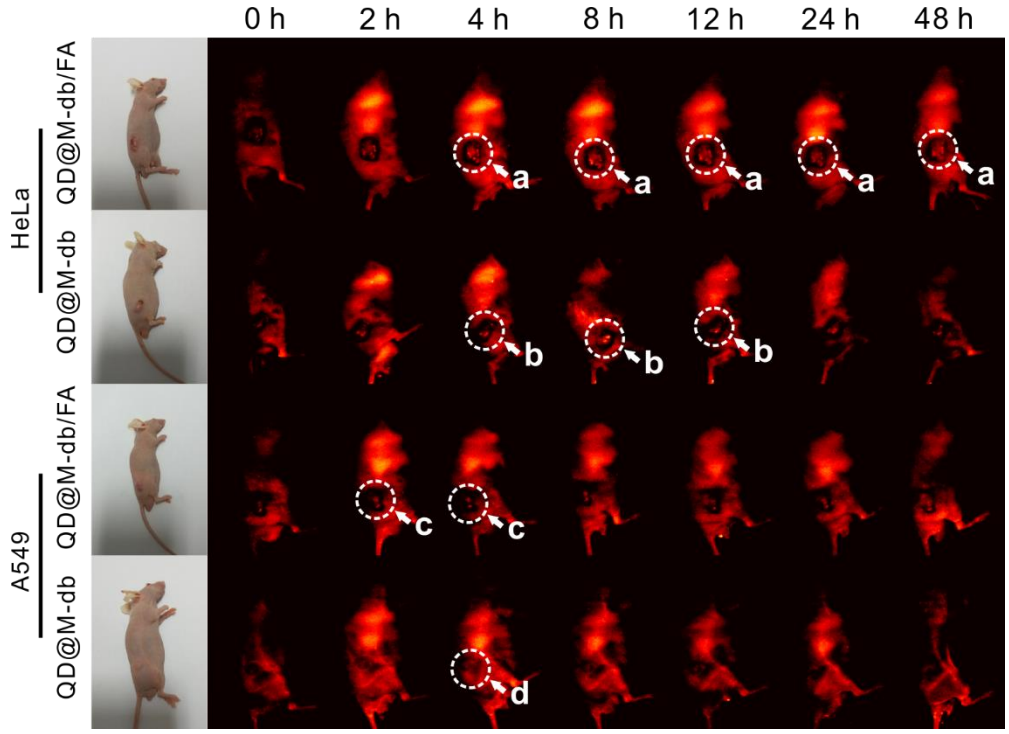

Figure S11. Fluorescence imaging at different time points after tail vein injection of QD@M-db/FA and QD@M-db in HeLa and A549 tumor-bearing nude mice (a, b, c and d indicated tumor sites, respectively).

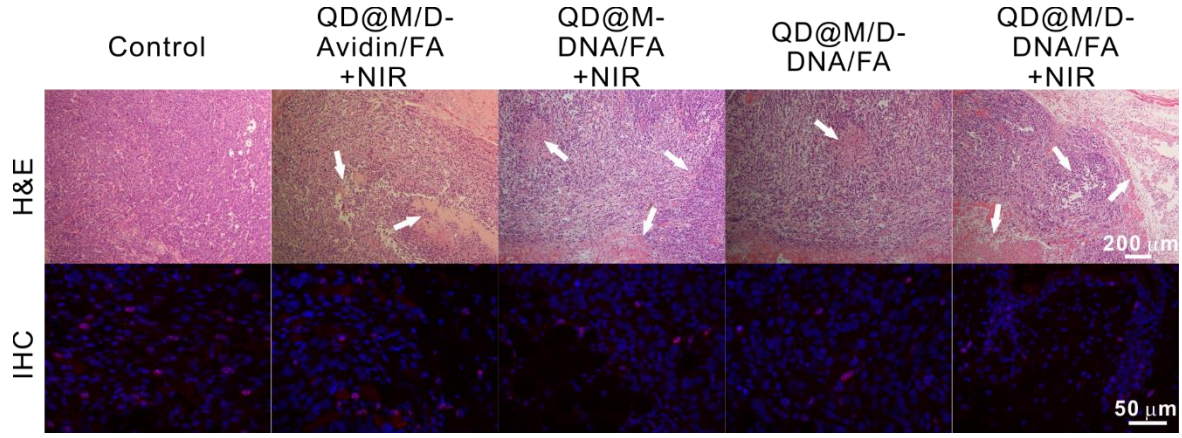

Figure S12. H&E and IHC staining of tumor from HeLa tumor-bearing nude mice with different treatments; necrotic tumor cells are labeled with white arrows.

References

1. Wang K, Wang Q, Luo Q, Yang X. Fluorescence molecular tomography in the second near-infrared window. Opt Express. 2015; 23: 12669-79.